# Low-Complexity Linear and Non-Linear Digital Self-Interference Cancellation

Muhammad Nabeel*, Akram Chbib*, Muhammad Sohaib Amjad†, Falko Dressler†, Jürgen Peissig*
*Leibniz Universität Hannover, Germany
†Technische Universität Berlin, Germany
Corresponding Author: Muhammad Nabeel (nabeel@ccs-labs.org)

***Abstract*—To fully utilize the in-band full-duplex (IBFD) communication in practice, digital self-interference (SI) cancellation is indispensable. In the literature, several methods have been proposed to suppress the SI signal in digital domain, however, mostly linear and non-linear SI techniques are studied separately. In this work, we review existing digital SI cancellation methods and present a low-complexity solution for both linear and non-linear digital SI cancellation by exploiting frequency-domain processing as well as a neural network-based approach. We developed an orthogonal frequency division multiplexing (OFDM)-based IBFD transceiver in GNU Radio and use it in combination with USRP software-defined radios (SDRs) to experimentally demonstrate the performance in an unified framework. Our results show that the proposed SI cancellation is computationally 4 times more efficient and achieves a similar SI cancellation performance as the state of the art.**

## I. Introduction

The in-band full-duplex (IBFD) communication is the key to doubling the spectral efficiency by re-using the available spectrum; it is considered a potential candidate for future sixth generation (6G) technology [1]. In fifth generation (5G) technology, the advantage offered by the IBFD is not fully utilized as the transceivers operate in frequency division duplex (FDD) or time division duplex (TDD) mode to avoid self-interference (SI). The SI signal, i.e., the signal received due to transceiver's own transmission, is one of the main reasons that makes the IBFD communication hard to achieve. In theory, SI cancellation should be simple as the transceiver is aware of the actual transmitted signal, however, in practice it is not straightforward due to the non-linearities introduced by the hardware components as well as the unknown channel between the transmit and receive antennas [2], [3].

In practical systems, SI cancellation is performed by suppressing the SI signal at different stages of the receive chain, i.e., passive, analog, and digital cancellation. Passive cancellation does not involve any adaptive tuning and is accomplished by choosing the right antenna configuration and structure, shielding, or isolation of transmit and receive paths. Active analog cancellation is usually achieved by using a tunable radio frequency (RF) circuit that transforms the known transmitted signal into expected SI signal, which is then subtracted from the actual received signal. Since it is impossible in practice to construct a perfect SI signal due to the involved hardware components, there is still a residual SI signal that needs to be suppressed by using digital cancellation.

The residual SI signal is composed of two parts: linear and non-linear. The linear part of the SI signal is directly related to the transmit power. Hence, it is easier to suppress than the non-linear SI signal which is caused by the power amplifier (PA), digital-to-analog converter (DAC), and in-phase and quadrature (IQ) imbalance of the transceiver. Comparatively, the linear part is also the dominant one, however, the cancellation of non-linear SI signal is still necessary especially when the signal of interest (SoI) has a very low power. For example, in the case of joint communication and sensing (JCAS) in 6G, the SoI is not only several orders of magnitude weaker, but also highly correlated with the SI signal making the non-linear SI cancellation crucial [4]. For linear SI cancellation, the receiver first estimates the channel between the transmit and receive antennas of the transceiver by using the training data before the DAC. Afterwards, this estimation is used to reconstruct a SI signal copy, which is then subtracted from the received signal [5]. For non-linear SI cancellation, the non-linearity introduced by the hardware impairments is typically modelled using polynomials [6], [7]. Recently, it has been shown that these non-linear effects can also be modeled by using neural network (NN)-based approaches [8].

In this work, we investigate state-of-the-art digital SI cancellation methods and present a low-complexity solution for linear and non-linear digital SI cancellation by exploiting frequency-domain processing as well as a NN-based model. To demonstrate the performance of different digital SI cancellation methods, we developed an orthogonal frequency division multiplexing (OFDM)-based IBFD transceiver in GNU Radio and use universal software radio peripheral (USRP)-based software-defined radios (SDRs) for over-the-air experiments. Our results show that the presented SI cancellation is computationally more efficient and achieves a similar performance as the state of the art.

Our main contributions can be summarized as follows:

- We review existing SI cancellation methods and present a computational efficient solution for both linear and non-linear digital SI cancellation (Sections II and III).
- We develop an OFDM-based IBFD transceiver in GNU Radio and use it together with a SDR for over-the-air experiments in a lab environment (Section IV).
- We analyze the performance of presented digital SI cancellation methods in an unified framework (Section V).

## II. Related Work

In the IBFD systems, the SI signal can be up to 100 dB stronger than the SoI, therefore, it is difficult to eliminate the SI signal completely in a single stage, hence, SI cancellation is performed at different stages in the transceiver [2]. The most simplest of these is the passive cancellation that involves procedures such as the optimal placement of the transmit and receive antennas. Passive cancellation has the ability to suppress a huge part of the SI signal, however, the suppression achieved depends upon several factors including carrier frequency, bandwidth, antenna type and configuration [9]. Therefore, further suppression of the residual SI signal is required in the next stages.

In the case of multiple-input-multiple-output (MIMO) communication systems, beamforming can be exploited to have nulls at the receiving side of the transceiver for minimizing the SI [10]. This method is known as null-space projection (NSP) in the literature. When beamforming is not possible such as in the case of single-input-single-output (SISO) communication systems, active analog cancellation usually performed by tunable RF circuit is more common, however, it comes with an extra cost and higher complexity [11].

Finally, the residual SI signal that can be a few tens of dB is suppressed by using digital cancellation methods [4]. In the literature, the linear part of the digital SI signal is cancelled by using least square (LS), least minimum mean square error (LMMSE), or fast fourier transform (FFT) based methods. It is a common practice to exploit these methods, and perform the SI signal estimation and reconstruction in time domain [10], [12], [13]. However, it has been shown that realizing the digital SI cancellation in frequency domain offers improved performance especially in harsh channel conditions [5].

The non-linear part of the digital SI signal is typically cancelled by using the polynomial method [7], [14]. The polynomial method provides a good approximation of the non-linearity, however, the computational complexity is often high and it increases further with the increase in the maximum considered non-linearity order. As an alternate solution, recently neural networks are used to perform non-linear SI cancellation [8]. Even though there is a rich literature on digital SI cancellation, the linear and non-linear digital SI cancellation methods are mostly studied separately. Therefore, in this work, we investigate computational efficient implementation of both linear and non-linear digital SI cancellation in an unified framework. We analyze the performance in simulations and with over-the-air measurements by using a SDR that is readily available and is widely used in the academic community for testing the performance of new signal processing algorithms and wireless standards.

## III. Digital Self-Interference Cancellation

Figure 1 shows an IBFD transceiver with different stages of SI cancellation. Let us represent the digital baseband time-domain signal before the DAC, mixer, and PA by $x[n]$, where $n$ is the sample index. If $s[n]$ is the SoI and $w[n]$ is the additive white gaussian noise (AWGN) with zero mean and variance

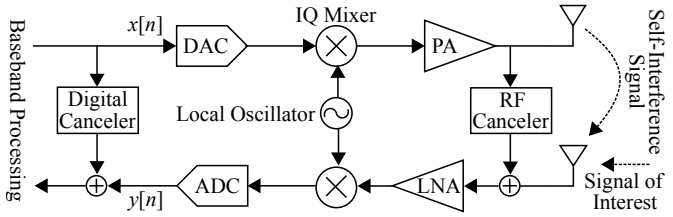


Figure 1: An in-band full-duplex transceiver with different stages of self-interference cancellation. Only relevant components are shown for clarity.

$\sigma^2$, the digital baseband time-domain received signal after the analog-to-digital converter (ADC) $y[n]$ without considering the non-linear hardware impairments is written as

$$y[n] = \sum_{l=0}^{L-1} h[l]x[n-l] + s[n] + w[n]. \tag{1}$$

Here, $h[l]$ denotes the channel impulse response (CIR) including other memory effects with maximum length $L$ and $l \in \{0, 1, ..., L-1\}$. We assume that this maximum length $L$ is equivalent to the cyclic prefix (CP) of an OFDM symbol and there are $N$ number of samples per OFDM symbol (which is also same as FFT size $K$). For the sake of simplicity, we also assume that there is no SoI $s[n]$, hence, $y[n]$ corresponds to the SI signal. From practical point of view, there is no difference as in presence of the SoI, the receiver will consider it as an interference for the training samples.

The main goal in the receiver chain is to estimate the CIR and reconstruct $y[n]$ by using known $x[n]$ so that the SI is eliminated completely. This SI signal in the digital domain is composed of two parts, linear denoted by $y_{lin}[n]$ and non-linear $y_{nl}[n]$. The linear part dominates the SI signal, however, as mentioned earlier, to fully exploit the IBFD technology, cancellation of non-linear part is also necessary.

### A. Linear Self-Interference Cancellation

For linear SI cancellation, here we focus only on least square estimation and reconstruction in time domain or in frequency domain, as they are comparatively simple to realize and outperform other known techniques.

*1) Time-Domain Linear Cancellation (TDLC):* In matrix and vector notation, the time-domain convolution operation can be equivalently replaced by a matrix multiplication, hence, vector $y$ representing the received signal samples in absence of the SoI can be re-written from (1) as

$$y = \mathbb{X}h + w. \tag{2}$$

Here, $\mathbb{X}$ is a Toeplitz matrix of a Circulant kind and of order $N \times L$ corresponding to the total number of training samples per OFDM symbol and the maximum length of CIR that can be estimated, respectively. Whereas, $h$ denotes a vector representing the CIR and vector $w$ corresponds to the noise added to each transmitted signal sample. The estimated CIR $\hat{h}$ is then computed by using the LS time-domain estimation as

$$\hat{h} = \mathbb{X}^{\dagger} y. \tag{3}$$

Here, $\mathbb{X}^{\dagger}$ denotes the Moore-Penrose (pseudo) inverse of the matrix $\mathbb{X}$. To reconstruct the received symbol, the estimated CIR $\hat{h}$ is convolved with the known transmitted symbol. This constructed symbol is then subtracted from the received symbol to finally realize the linear SI cancellation.

*2) Frequency-Domain Linear Cancellation (FDLC):* For the frequency-domain estimation and reconstruction, the received signal first undergoes the FFT operation. The received signal $Y[k]$ at $k_{th}$ subcarrier where $k \in \{0, 1, ..., K-1\}$ after the FFT operation is written as

$$Y[k] = X[k]H[k] + W[k]. \tag{4}$$

Here, $X[k]$, $H[k]$, and $W[k]$ represent the known transmitted signal, channel response, and additive noise all at the $k_{th}$ subcarrier, respectively. The estimated channel response $\hat{H}[k]$ at $k_{th}$ subcarrier is then obtained by using the LS frequency domain based estimation as

$$\hat{H}[k] = \frac{Y[k]}{X[k]}, \tag{5}$$

or equivalently

$$\hat{H} = diag(\mathbf{X})^{-1}Y. \tag{6}$$

Here, $\hat{H}$ and $Y$ are vectors representing the channel estimates and the transmitted signal over all subcarriers, respectively. Moreover, $diag(\mathbf{X})^{-1}$ denotes an inverse of a square matrix with known transmissions at each subcarrier of a symbol in the diagonal. The product of the obtained channel estimate and the known transmitted signal is then used to obtain the reconstructed signal at each subcarrier. Finally, inverse fast fourier transform (IFFT) is performed on the reconstructed signal to transform it into time domain for realizing the linear SI cancellation.

### *B. Non-Linear Self-Interference Cancellation*

Considering the reconstructed signal using linear SI techniques $\hat{y}_{lin}[n]$ is ideal, the residual received signal now consists of only non-linear part as

$$y_{nl}[n] \approx y[n] - \hat{y}_{lin}[n]. \tag{7}$$

This non-linearity is mainly introduced by the transmitter IQ imbalance and is further enhanced by the PA especially when the transmitter and receiver chains use the same local oscillator as is the case of IBFD. In the literature, the non-linearity is modeled by using a polynomial method. The polynomial method and non-linear SI cancellation by using a neural network are discussed in the next sub-sections.

*1) Polynomial Non-Linear Cancellation (PNLC):* Without the SoI $s[n]$ and considering $w[n]$ as negligible, (1) with introduced non-linear behaviour can be re-written as [7], [8]

$$y[n] = \sum_{\substack{a=1 \\ a\ odd}}^{A} \sum_{b=0}^{a} \sum_{l=0}^{L-1} h_{a,b}[l]x[n-l]^b x^*[n-l]^{a-b}. \tag{8}$$

Here, $x^*[.]$ refers to the complex conjugate of the transmitted signal samples, parameter $h_{a,b}[l]$ includes the joint effect of CIR, IQ imbalance parameters, and PA non-linearity of order $a \in \{1, 3, ..., A\}$, whereas the memory length of PA is included in the maximum considered length $L$. The even values of $a$ are not considered as they are usually filtered out by the band-pass filters of the transceiver. It can be noted that considering $a = 1$, $b = 1$, (8) will be equivalent to (1). To eliminate the non-linear SI signal, the idea is to estimate all coefficients $h_{a,b}[l]$ by using a LS method similar to as described for the linear SI cancellation and reconstruct $y_{nl}[n]$ for subtraction. The computational complexity of this method increases with the increase in the non-linearity order.

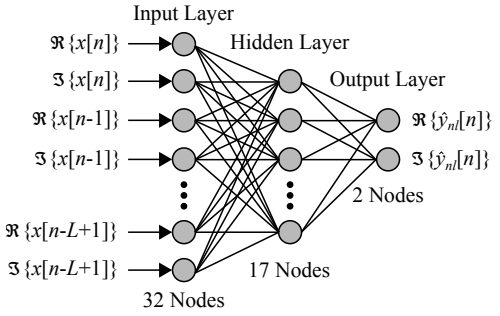


Figure 2: A feed-forward neural network for the estimation of non-linear self-interference signal.

*2) Neural Network Non-Linear Cancellation (NNLC):* Instead of computing the coefficients, the idea with neural networks is to reconstruct the residual non-linear part in the received signal $y_{nl}[n]$ directly from the transmitted signal samples $x[n]$. Figure 2 shows a feed-forward neural network with three layers, i.e., input, hidden, and output. The input layer has $2L$ nodes corresponding to the real (denoted by $\Re$) and imaginary (denoted by $\Im$) parts of $x[n]$ as separate entries along with its $L-1$ delayed versions that are related to the current $y_{nl}[n]$. The hidden layer has $N_h$ nodes, whereas the output layer has two nodes for real and imaginary parts of $y_{nl}[n]$. In general, the output of the nodes in a layer denoted by vector $I$ is obtained by applying the activation function $f(.)$ on the weighted sum of the output of nodes from the previous layer $\mathbf{W}I_0$ and the nodes bias as

$$I = f(\mathbf{W}I_0 + bias). \tag{9}$$

Here, size of both vectors $I$ and $bias$ is equivalent to the total number of nodes in the current layer, size of vector $I_0$ is equivalent to the total number of nodes in the previous layer, and $\mathbf{W}$ is a matrix of order equivalent to number of nodes in current layer by number of nodes in the previous layer. It is important to highlight that here we consider only one hidden layer, however, one can choose any number of hidden layers and nodes with an expense of increased computational complexity. The output of a node in any hidden layer will depend upon the output of the nodes in the previous layer similar to as described by (9). Nevertheless, regardless of the neural network structure, the main goal is to use $N$ number of training samples and minimize the mean squared error (MSE) between the expected output $y_{nl}[n]$ and the actual

output $\hat{y}_{nl}[n]$ as

$$MSE = \frac{1}{N}\sum_{n=0}^{N-1}(\Re\{y_{nl}[n]\} - \Re\{\hat{y}_{nl}[n]\})^2 + \frac{1}{N}\sum_{n=0}^{N-1}(\Im\{y_{nl}[n]\} - \Im\{\hat{y}_{nl}[n]\})^2. \quad (10)$$

To minimize the MSE, the neural network exploits back-propagation and converges towards the optimum values for $\mathbf{W}$ and *bias*. Once the neural network is trained, it is then able to predict $\hat{y}_{nl}[n]$ for any new input.

It is interesting to note that using a neural network for the non-linear digital SI cancellation does not follow the conventional approach of estimating and reconstructing the signal separately, hence, reducing the overall computational complexity. Moreover, it is also worth mentioning that here we exploit the neural network only for the non-linear digital SI cancellation. Using neural networks is not beneficial for the linear part as simple LS methods discussed in the previous sub-sections already provide the least complexity. Furthermore, for simplicity, the neural network used here exploits only the time-domain signal for non-linear digital SI cancellation and utilizing the frequency-domain signal is left for a future work.

### C. Computational Complexity

To compare the computational complexity of the presented SI cancellation methods, we focus on the required real-valued multiplications and real-valued additions. We assume that one complex multiplication requires four real multiplications and two real additions, whereas one complex addition requires two real additions. It is important to highlight that in this work we do not consider Gauss algorithm that focuses on reducing the number of real multiplications required to perform a complex multiplication as it will not affect the relative performance.

*1) Linear Self-Interference Cancellation:* Each considered linear SI cancellation method has two main processing parts, i.e., channel estimation and signal reconstruction using that estimation. For TDLC estimation, the computations required per symbol are calculated from (3). Since the matrix obtained for the transmitted training samples is computed in advance, the main computations depend upon the number of samples per symbol and the CIR length. For reconstruction, we rely upon circular convolution based algorithm that utilizes FFT and IFFT to optimize the overall complexity [5]. We exploit Radix-2 processing for the N-point FFT and the IFFT operation which requires $(N/2)log_2N$ complex multiplications and $Nlog_2N$ complex additions. Contrary, for the FDLC estimation, first a single FFT operation is required before computing per subcarrier estimate. Next, IFFT operation is realized to convert the signal into time domain after frequency-domain equalization. The computational complexity of the presented digital SI cancellation methods is summarized in Table I. For TDLC and FDLC, the first term shows the computational complexity for the estimation part, whereas the second term is related to the reconstruction.

TABLE I: Computational Complexity for Self-Interference Cancellation.

| | Real Multiplications | Real Additions |
|---|---|---|
| **TDLC** | $(4NL)+$ $(6Nlog_2N - 17N + 36)$ | $(4NL)+$ $(9Nlog_2N - 7N + 12)$ |
| **FDLC** | $(2Klog_2K - 7K + 12)+$ $(2Klog_2K - 3K + 12)$ | $(3Klog_2K - 3K + 4)+$ $(3Klog_2K - K + 4)$ |
| **PNLC** | $L(A + 1)(A + 3)$ | $L(A + 1)(A + 3)$ |
| **NNLC** | $(2L + 2)N_h$ | $(2L + 3)N_h$ |

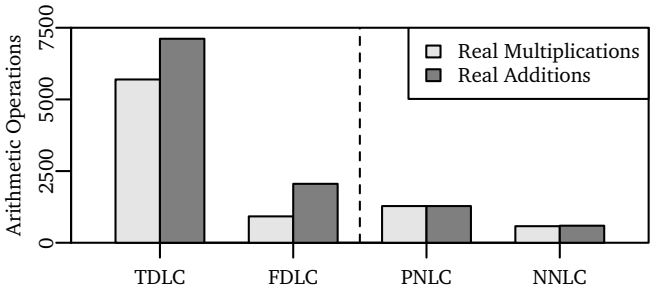


Figure 3: Arithmetic operations required for self-interference cancellation.

*2) Non-Linear Self-Interference Cancellation:* For the non-linear SI cancellation using PNLC and NNLC, it is important to carefully select the polynomial order, i.e., the non-linearity order $A$, and the number of hidden layers and nodes as they directly contribute towards the overall computational complexity. To have a fair comparison, we select them in a way so that both methods provide a similar performance. We realize PNLC by using a polynomial order of 7. The computations required for the polynomial basis functions are not considered as the processing required is comparatively negligible [8]. Moreover, we also ignore the channel estimation complexity for the PNLC which is similar to as described for the linear SI cancellation and if considered will further increase the required processing. In the case of NNLC, we exploit a neural network that has three layers, i.e., input, hidden, and output each having 32, 17, and 2 nodes, respectively. We assume that the used activation function, i.e., ReLU, has a similar complexity as a single real-valued addition, hence, the overall computational complexity can be obtained together from (9). Moreover, we ignore the processing required for the training of the neural network as it is usually done only once in the calibration phase. The computational complexity required per sample for the aforementioned non-linear digital SI cancellation methods is also summarized in Table I. Whereas, the exact number of real additions and real multiplications required per symbol with $N = K = 64$ and $L = 16$ for linear SI cancellation, and per sample with $A = 7$ and $N_h = 17$ for non-linear SI cancellation are depicted in Figure 3. It can be noted that the FDLC is around four times less computational complex than the TDLC, whereas NNLC involves two times less computational complexity than the PNLC.

## IV. Implementation Details

To demonstrate the performance of IBFD digital cancellation, we have developed an OFDM-based transceiver in GNU Radio. GNU Radio is an Open Source SDR platform that offers signal processing modules implemented in software

Figure 4: Experimental setup showing USRP device and aluminium foil between its transmit and receive antenna for passive SI suppression.

(using Python/C++) in form of blocks connected together to realize their real-time operation on a host PC. For assessing the performance in simulations, GNU Radio offers channel model blocks that allow to configure noise power, multipath, etc. Whereas, for over-the-air testing, the PC can be connected to an USRP device which performs DAC/ADC and frequency up-conversion/downconversion before transmitting/receiving the signal via antennas.

### A. OFDM Generation and Transmission

The communication is frame based where OFDM frame structure follows the IEEE 802.11a/g standard similar to as described in [15], [16]. The training symbols are modulated with binary phase shift-keying (BPSK), whereas the data symbols are quadrature phase shift-keying (QPSK) modulated. Each OFDM symbol is composed of 48 data subcarriers and 4 pilots, and has a signal bandwidth of 16.6 MHz. The subcarrier spacing is 312.5 kHz and a time-domain OFDM symbol is obtained by applying the IFFT operation followed by the addition of 16 samples CP resulting in a symbol duration of 4 µs including CP. The final signal is then passed through a wireless channel block in simulations or transmitted in 2.4 GHz band by using the transmit antenna of the N210 USRP device for over-the-air testing. The experimental setup including the used USRP device with aluminium foil between the transmit and receive antenna is shown in Figure 4. The experiments are performed in a controlled lab environment providing nearly static CIR throughout the experiments. Moreover, the aluminium foil is used for passive SI suppression and to bring the received signal power in the dynamic range of USRP ADC as we do not utilize any active analog SI cancellation. Along with propagation loss, our system achieves a passive suppression of more than 50 dB.

### B. Receiver Processing

The SI signal is received on the receiver side after the wireless channel block in simulations or via receive antenna of the USRP device. In the latter case, the received signal is first downconverted to baseband. The transmitted digital baseband time-domain signal is used as a reference to detect the beginning of each frame start at the receiver.

For TDLC, the estimation is performed directly on the time domain received signal, whereas for FDLC, 64-point FFT is applied before estimating and reconstructing the signal in frequency domain followed up by the IFFT processing. Next, non-linear cancellation is observed. For the implementation of PNLC and NNLC, we consider the polynomial order and the number of hidden layers and nodes same as described in the previous section. Moreover, for the training of the neural network, we divide the whole data into two parts, i.e., 90 % for training and 10 % for testing with a mini-batch size of 32 and a learning rate of 0.004. Finally, ReLU is used as an activation function for the hidden layer and a linear activation function for the output layer.

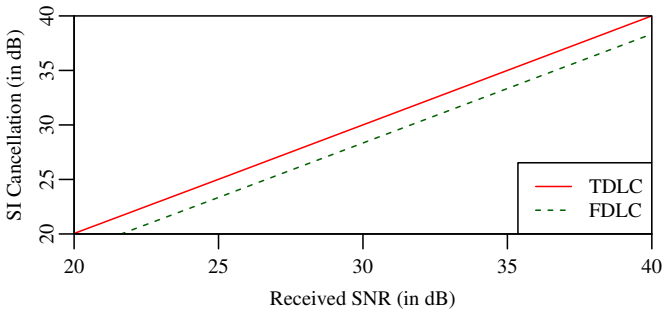


Figure 5: Linear self-interference cancellation over an AWGN channel.

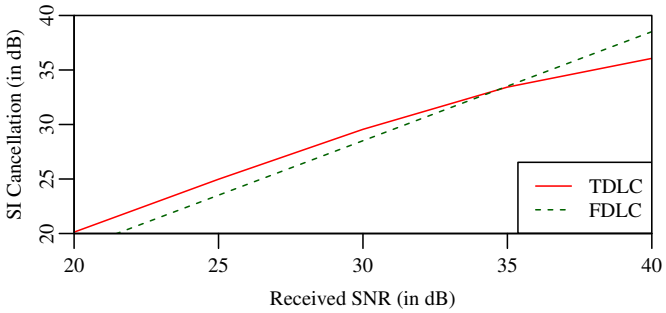


Figure 6: Linear self-interference cancellation over frequency-selective fading.

## V. Results and Discussion

To have a baseline SI cancellation performance, first we compare the TDLC and FDLC in simulations without introducing any non-linear effect. The resultant linear cancellation over different received signal-to-noise ratio (SNR) values in presence of an AWGN channel is shown in Figure 5. It can be observed that the SI cancellation is linear over the considered SNR range, hence, validating the implementation. Moreover, it can be noted that the linear cancellation in TDLC performs around 1.5 dB better than the FDLC in the case of AWGN channel. However, when we consider frequency-selective fading, the performance of TDLC starts degrading especially for the higher SNR values, whereas performance of FDLC remains linear as shown in Figure 6. This is because of the fact that the channel estimate per subcarrier is still accurate in the case of frequency-selective fading. Hence, it can be concluded that even though FDLC performs marginally worse than the TDLC, the FDLC is superior to TDLC in the complex scenarios. Furthermore, the FDLC achieves this performance comparatively with a much lower computational complexity.

Next, we perform over-the-air experiments with an USRP N210 device, hence, non-linearity is introduced by its hard-

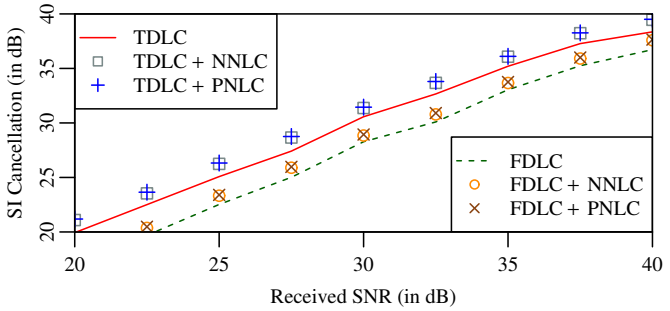


Figure 7: Linear and non-linear self-interference cancellation with over-the-air measurements.

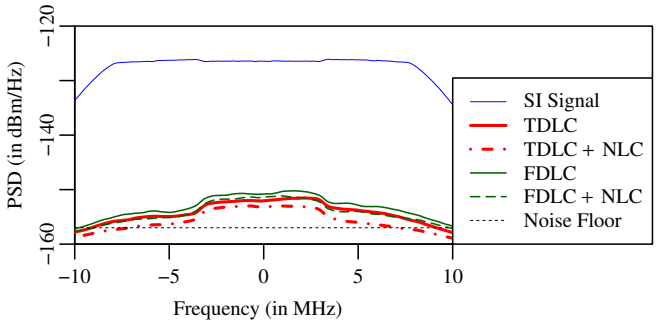


Figure 8: Power spectral density before and after linear and non-linear self-interference cancellation.

ware impairments. To perform the measurements in a controlled lab environment, we use the setup shown in Figure 4. Since we cannot easily measure the absolute transmit power, thus we focus on the relative increase. Figure 7 shows the performance with different linear and non-linear SI cancellation methods. It can be noted that the relative performance of TDLC and FDLC is similar to what is observed in simulations for the AWGN channel. For high SNR values, the trend is not completely linear due to the non-linearity introduced by the hardware impairments. Moreover, the relative improvement with non-linear SI cancellation is more than 1 dB and is same for both PNLC and NNLC regardless of whether TDLC or FDLC was used for linear SI cancellation. Hence, it is clear that using a neural network does not degrade the performance and at the same time keeps the computational complexity low. It is important to mention that the non-linearity introduced by the USRP for the considered SNR range seems only marginal, however, it is good enough to compare the relative performance as the focus here is not on the absolute improvement.

Finally, we plot the power spectral density (PSD) before and after SI cancellation for a single SNR measurement in Figure 8. For the sake of clarity, we do not plot PNLC and NNLC separately because both achieve a similar performance as also noted in the previous figure, therefore, represent them by a non-linear cancellation (NLC). The SI signal in the figure is the power received at the receiving side of the transceiver after the propagation loss and considered passive cancellation. Moreover, the average noise floor is represented by a horizontal dashed line. It can be seen that our system is able to achieve an overall digital SI cancellation of more than 20 dB with the considered hardware setup.

## VI. Conclusion

In this work, we focused on investigating the low-complexity solution for both linear and non-linear digital SI cancellation. To analyze the performance, we developed an OFDM based IBFD transceiver in an SDR platform. Our results reveal that using frequency domain processing for linear SI cancellation together with a neural network based model for non-linear SI cancellation reduce the overall computational complexity up to 4 times. This improvement is observed with only a marginal degradation in the overall performance.

## References


[1] X. Lin, "An Overview of 5G Advanced Evolution in 3GPP Release 18," *IEEE Communications Standards Magazine*, vol. 6, no. 3, pp. 77–83, Sep. 2022.

[2] C. D. Nwankwo, L. Zhang, A. Quddus, M. A. Imran, and R. Tafazolli, "A Survey of Self-Interference Management Techniques for Single Frequency Full Duplex Systems," *IEEE Access*, vol. 6, pp. 30 242–30 268, May 2018.

[3] M. Erdem, O. Gurbuz, and H. Ozkan, "Integrated Linear and Nonlinear Digital Cancellation for Full Duplex Communication," *IEEE Wireless Communications*, vol. 28, no. 1, pp. 20–27, 2021.

[4] C. B. Barneto, T. Riihonen, M. Turunen, L. Anttila, M. Fleischer, K. Stadius, J. Ryynänen, and M. Valkama, "Full-Duplex OFDM Radar with LTE and 5G NR Waveforms: Challenges, Solutions, and Measurements," *IEEE Transactions on Microwave Theory and Techniques*, vol. 67, no. 10, pp. 4042–4054, 2019.

[5] M. S. Amjad, H. Nawaz, K. Ozsoy, O. Gurbuz, and I. Tekin, "A Low-Complexity Full-Duplex Radio Implementation With a Single Antenna," *IEEE Transactions on Vehicular Technology*, vol. 67, no. 3, pp. 2206–2218, Mar. 2018.

[6] L. Anttila, D. Korpi, E. Antonio-Rodriguez, R. Wichman, and M. Valkama, "Modeling and efficient cancellation of nonlinear self-interference in MIMO full-duplex transceivers," in *IEEE GLOBECOM 2014, Wi5G Workshop*. IEEE, Dec. 2014, pp. 777–783.

[7] D. Korpi, L. Anttila, and M. Valkama, "Nonlinear self-interference cancellation in MIMO full-duplex transceivers under crosstalk," *Journal on Wireless Communications and Networking*, vol. 2017, pp. 1–15, 2017.

[8] Y. Kurzo, A. T. Kristensen, A. Burg, and A. Balatsoukas-Stimming, "Hardware Implementation of Neural Self-Interference Cancellation," *IEEE Journal on Emerging and Selected Topics in Circuits and Systems*, vol. 10, no. 2, pp. 204–216, 2020.

[9] Y. Chen, C. Ding, Y. Jia, and Y. Liu, "Antenna/propagation domain self-interference cancellation (SIC) for in-band full-duplex wireless communication systems," *Sensors*, vol. 22, no. 5, p. 1699, 2022.

[10] M. A. Ahmed, C. C. Tsimenidis, and A. F. Al Rawi, "Performance analysis of full-duplex-MRC-MIMO with self-interference cancellation using null-space-projection," *IEEE Transactions on Signal Processing*, vol. 64, no. 12, pp. 3093–3105, 2016.

[11] J. W. Kwak, M. S. Sim, I.-W. Kang, J. Park, K.-K. Wong, and C.-B. Chae, "Analog self-interference cancellation with practical RF components for full-duplex radios," *IEEE Transactions on Wireless Communications*, 2022.

[12] D. Bharadia, E. McMilin, and S. Katti, "Full Duplex Radios," *ACM SIGCOMM Computer Communication Review*, vol. 43, no. 4, pp. 375–386, Oct. 2013.

[13] D. Korpi, L. Anttila, V. Syrjälä, and M. Valkama, "Widely linear digital self-interference cancellation in direct-conversion full-duplex transceiver," *IEEE Journal on Selected Areas in Communications*, vol. 32, no. 9, pp. 1674–1687, Sep. 2014.

[14] M. S. Sim, M. Chung, D. Kim, J. Chung, D. K. Kim, and C.-B. Chae, "Nonlinear self-interference cancellation for full-duplex radios: From link-level and system-level performance perspectives," *IEEE Communications Magazine*, vol. 55, no. 9, pp. 158–167, 2017.

[15] B. Bloessl, M. Segata, C. Sommer, and F. Dressler, "An IEEE 802.11a/g/p OFDM Receiver for GNU Radio," in *ACM SIGCOMM 2013, SRIF Workshop*. ACM, Aug. 2013, pp. 9–16.

[16] M. S. Amjad and F. Dressler, "Software-based Real-time Full-duplex Relaying: An Experimental Study," *IEEE Transactions on Green Communications and Networking*, vol. 4, no. 3, pp. 647–656, Sep. 2020.